The effect of a magnetic field on a 2D problem of fibre-reinforced thermoelasticity rotation under three theories

Kh. Lotfy[a)b)†]

[a)] *Department of Mathematics, Faculty of Science, Zagazig University, Zagazig, P. O. Box* 44519, *Egypt*

[b)] *Department of Mathematics, Faculty of Science and Arts, Al-mithnab, Qassim University, P. O. Box* 931, *Buridah* 51931, *Al-mithnab, Kingdom of Saudi Arabia*

(Received 26 November 2011; revised manuscript received 26 November 2011)

In the present paper, we introduce the coupled theory (CD), Lord–Schulman (LS) theory, and Green–Lindsay (GL) theory to study the influences of a magnetic field and rotation on a two-dimensional problem of fibre-reinforced thermoelasticity. The material is a homogeneous isotropic elastic half-space. The method applied here is to use normal mode analysis to solve a thermal shock problem. Some particular cases are also discussed in the context of the problem. Deformation of a body depends on the nature of the force applied as well as the type of boundary conditions. Numerical results for the temperature, displacement, and thermal stress components are given and illustrated graphically in the absence and the presence of the magnetic field and rotation.

Keywords: Lord–Schulman theory, Green–Lindsay theory, coupled theory, reinforcement, rotation, magnetic field

PACS: 42.65.Hf **DOI:** 10.1088/1674-1056/21/6/064214

1. Introduction

The linear theory of elasticity is of paramount importance in the stress analysis of steel, which is the commonest engineering structural material. To a lesser extent, linear elasticity describes the mechanical behavior of the other common solid materials, e.g. concrete, wood, and coal. However, the theory does not apply to the behavior of many of the new synthetic materials of the clastomer and polymer type, e.g. polymethyl-methacrylate (Perspex), polyethylene, and polyvinyl chloride. The concept of using fibers as reinforcement is not new. Fibers have been used as reinforcement since ancient times. Historically, horsehair was used in mortar and straw in mud bricks. In the early 1900s, asbestos fibers were used in concrete, and in the 1950s the concept of composite materials came into being and fiber reinforced concrete was one of the topics of interest. There was a need to find a replacement for the asbestos used in concrete and other building materials once the health risks associated with the substance were discovered. By the 1960s, steel, glass, and synthetic fibers such as polypropylene fibers were used in concrete, and the research into new fiber-reinforced concretes continues today. A reinforced concrete should be designed for all conditions and stresses that may occur and accord with the principles of mechanics. Fiber-reinforced composites are used in a variety of structures due to their low weight and high strength. The characteristic property of a reinforced composite is that its components act together as single anisotropic units as long as they remain in the elastic condition. The wave propagation in a reinforced medium plays a very interesting role in civil engineering and geophysics. The studies of propagation, reflection, and transmission of waves are of great interest to seismologists. Such studies help them to obtain knowledge about the rock structures as well as their elastic properties and at the same time information regarding minerals and fluids present inside the earth.

The investigation of interaction between a magnetic field, stress, and strain in a thermoelastic solid is very important due to its many applications in the fields of geophysics, plasma physics, and relevant topics, especially in the nuclear field, where the extremely high temperature and temperature gradients, as well as the magnetic fields originating in-

†Corresponding author. E-mail: khlotfy_1@yahoo.com

© 2012 Chinese Physical Society and IOP Publishing Ltd

side nuclear reactors, influence their design and operation. The theory of magneto-thermoelasticity is concerned with the influence of a magnetic field on the elastic and thermoelastic deformations of a solid body. This theory has aroused much interest in recent years, because of its applications in various branches of science and technology. The development of interaction of electromagnetic field, the thermal field, and the elastic field are available in many papers.[1−3] The idea of introducing a continuous self-reinforcement at every point of an elastic solid was given by Belfied *et al.*[4] The model was later applied to the rotation of a tube by Verma and Rana.[5] Singh[6] showed that for wave propagation in a fibre-reinforced anisotropic medium, this decoupling cannot be achieved by the introduction of the displacement potential. Sengupta and Nath[7] discussed the problem of the surface waves in fibre-reinforced anisotropic elastic media. Hashin and Rosen[8] gave the elastic moduli for fibre-reinforced materials. The problem of plane-wave reflection at the free surface of a fibre-reinforced elastic half-space was discussed by Singh B and Singh S J.[9] Chattopadhyay and Choudhury[10] have discussed the problems of propagation, reflection, and transmission of magnetoelastic shear waves in a self-reinforced medium. The reflection and the transmission of plane SH wave through a self-reinforced elastic layer sandwiched between two homogeneous visco-elastic solid half-spaces have been studied by Chaudhary *et al.*[11] Chattopadhyay and Chaudhary[12] studied the propagation of magneto-elastic shear waves in an infinite self-reinforced plate. Pradhan *et al.*[13] studied the dispersion of Loves waves in a self-reinforced layer over an elastic non-homogenous half-space. The propagations of plane waves in fibre-reinforced media were discussed by Chattopadhyay *et al.*[14] Othman and Song[15] showed the effects of initial stress, thermoelastic parameter, and thermal boundary condition on the reflection amplitude ratio. The problem of magneto-elastic transverse surfaces waves in self-reinforced elastic solid was studied by Verma *et al.*[16] The problem of wave propagation in thermally conducting linear fibre-reinforced composite materials was discussed by Singh.[17] The influence of an external magnetic field on the propagation of purely transverse waves polarized to the plane faces in a homogeneous, initially unstressed, infinitely conducting, self-reinforced elastic flat plate extending to infinity was studied by Verma.[18] Ezzat and Othman[19] have studied a two-dimensional (2D) magneto-thermoelasticity plane waves with thermal relaxation in non-rotating medium of perfect conductivity, a 2D electro-magneto-thermoelastic problem was dealt with for a finitely conducting half-space by Sherief and Helmy.[20] Roy Choudhuri and Mukhopadhyay[21] studied the propagation of electro-magneto-thermoelastic harmonic waves in an unbounded isotropic conducting medium permeating uniform field when the entire medium rotated with a uniform angular velocity. Othman *et al.*[22] formulated the magneto-thermoelastic coupled two-dimensional problem of a thermally and perfect conducting half-space solid in the presence of moving internal heat source. Ezzat and Othman[23] constructed a model of 2D equations of generalized magneto-thermoelasticity with two relaxation times in a perfectly conducting medium. In the context of the Green and Lindsay generalized thermoelasticity with two relaxation times, the problem of the propagation of electromagneto-thermoelastic disturbances produced by a thermal shock in a perfectly conducting elastic half-space was discussed by Othman.[24] Othman[25] has studied the problem of 2D electro-magneto-thermo-viscoelasticity for a thermally and electrically conducting half-space solid whose surface is subjected to a thermal shock with one relaxation time. Among the authors who considered the generalized magneto-thermoelasticity equation is Roy Choudhuri,[26] who extended these results to rotating media. The propagation of electromagnetic-thermoelastic disturbance produced by a thermal shock in a finitely conducting elastic half-space was investigated by Lotfy.[27] By using the Lord–Shulman theory, Roy Choudhuri and Debnath[28] studied the plane-wave propagations in infinite rotating media and in both thermoelastic and magneto thermoelastic media and also thermo-viscoelasticity. Othman and Lotfy[29] studied a 2D problem of generalized magneto-thermoelasticity under the effect of temperature dependent properties. Lotfy[30] studied microstretch in a half-space under generalized thermoelasticity with mode I crack. Othman and Lotfy[31] studied the plane waves in a generalized thermo-microstretch elastic half-space by using a general model of the equations of generalized thermo-microstretching for a homogeneous isotropic elastic half-space. Othman and Lotfy[32] studied the generalized thermo-microstretch elastic medium with temperature-dependent properties for different theories.

In the present investigation, we formulate the

fiber-reinforced 2D problem of thermoelasticity for an infinite space weakened by a finite linear opening, which is solved for the considered variables. The normal mode method is used to obtain the exact expressions for the considered variables. The distributions of the considered variables are represented graphically. Some particular cases are also derived from the present investigation.

2. Formulation of the problem and basic equations

We consider the problem of a thermoelastic half-space ($x \geq 0$). A magnetic field with constant intensity $\boldsymbol{H} = (0, 0, H_0)$, acting in the direction parallel to the boundary plane (taken as the direction of the z axis). The surface of the half-space is subjected to a thermal shock which is a function of y and t. Thus, all quantities considered will be functions of time variable t, and coordinates x and y. We begin our consideration with a linearized electro-dynamics slowly moving medium

$$\boldsymbol{J} = \operatorname{curl} \boldsymbol{h} - \varepsilon_0 \dot{\boldsymbol{E}}, \tag{1}$$

$$\operatorname{curl} \boldsymbol{E} = -\mu_0 \dot{\boldsymbol{h}}, \tag{2}$$

$$\boldsymbol{E} = -\mu_0 (\dot{\boldsymbol{u}} \times \boldsymbol{H}), \tag{3}$$

$$\boldsymbol{\nabla} \cdot \boldsymbol{h} = 0, \tag{4}$$

where μ_0 is the magnetic permeability, ε_0 is electric permeability and $\dot{\boldsymbol{u}}$ is the particle velocity of the medium, and the small effect of temperature gradient on $\boldsymbol{J}$ is also ignored.

These equations are supplemented by the constitutive equations for a fibre-reinforced linearly thermoelastic anisotropic medium with respect to the reinforcement direction $\boldsymbol{a}$ (Belfied *et al.*[4]) as follows:

$$\begin{aligned}\sigma_{ij} = {} & \lambda e_{kk}\delta_{ij} + 2\mu_T e_{ij} + \alpha(a_k a_m e_{km}\delta_{ij} + a_i a_j e_{kk}) \\ & + 2(\mu_L - \mu_T)(a_i a_k e_{kj} + a_j a_k e_{ki}) \\ & + \beta a_k a_m e_{km} a_i a_j - \gamma(T - T_0)\delta_{ij},\end{aligned} \tag{5}$$

where σ_{ij} are components of stress; e_{ij} are the components of strain; λ, μ_l are elastic constants; α, β, $(\mu_L - \mu_T)$ are the reinforcement parameters; $\gamma = (3\lambda + 2\mu)\alpha_t$ with α_t being the thermal expansion coefficient and $a \equiv (a_1, a_2, a_3)$, $a_1^2 + a_2^2 + a_3^2 = 1$. We choose the fibre-direction as $a \equiv (1, 0, 0)$. The strains can be expressed in terms of the displacement u_i as

$$e_{ij} = \frac{1}{2}(u_{i,j} + u_{j,i}). \tag{6}$$

For plane strain deformation in the x–y plane (5) then yields

$$\sigma_{xx} = A_{11}u,x + A_{12}v,y - \gamma(T - T_0), \tag{7}$$

$$\sigma_{yy} = A_{12}u,x + A_{22}v,y - \gamma(T - T_0), \tag{8}$$

$$\sigma_{zz} = A_{12}u,x + \lambda v,y - \gamma(T - T_0), \tag{9}$$

$$\sigma_{xy} = \mu_L(u,y + v,x), \quad \sigma_{xz} = \sigma_{yz} = 0, \tag{10}$$

where

$$\begin{aligned}A_{11} &= \lambda + 2(\alpha + \mu_T) + 4(\mu_L - \mu_T) + \beta, \\ A_{12} &= \alpha + \lambda, \quad A_{22} = \lambda + 2\mu_T.\end{aligned} \tag{11}$$

Since the medium is rotating uniformly with an angular velocity $\boldsymbol{\Omega} = \Omega\boldsymbol{n}$, where $\boldsymbol{n}$ is a unit vector representing the direction of the axis of rotation. The displacement equation of motion in the rotating frame of reference has two additional terms, centripetal acceleration, $\boldsymbol{\Omega} \times (\boldsymbol{\Omega} \times \boldsymbol{u})$ due to time-varying motion only and the Corioli's acceleration $2\boldsymbol{\Omega} \times \dot{\boldsymbol{u}}$ where $\boldsymbol{u}$ is the dynamic displacement vector. The equation of motion, taking into consideration the Lorentz force is

$$\begin{aligned}&\rho[\ddot{u}_i + \{\boldsymbol{\Omega} \times (\boldsymbol{\Omega} \times \boldsymbol{u})\}_i + (2\boldsymbol{\Omega} \times \dot{\boldsymbol{u}})_i] \\ &= \sigma_{ij,j} + \mu_0(\boldsymbol{J} \wedge H), \quad i, j, k = 1, 2, 3.\end{aligned} \tag{12}$$

The dynamic displacement vector is actually measured from a steady-state deformed position and the deformation is supposed to be small. Due to the application of the initial magnetic field $\boldsymbol{H}$, they result an induced magnetic field $\boldsymbol{h} = (0, 0, h)$ and an induced electric field $\boldsymbol{E}$, as well as the simplified equations of electro-dynamics of a slowly moving medium for a homogeneous, thermal and electrically conducting elastic solid.

The heat conduction equation in general formula is

$$\begin{aligned}kT_{,ii} = {} & \left(n_1 \frac{\partial}{\partial t} + \tau_0 \frac{\partial^2}{\partial t^2}\right) \rho C_E T \\ & + \gamma T_0 \left(n_1 \frac{\partial}{\partial t} + n_0 \tau_0 \frac{\partial^2}{\partial t^2}\right) u_{i,i},\end{aligned} \tag{13}$$

where ρ is the density, k is the thermal conductivity, C_E is the specific heat at constant strain and T is the temperature above reference temperature T_0, n_1, and n_0 are the parameters. In the above equations a dot denotes differentiation with respect to time, and comma followed by a subscript denotes partial differentiation with respect to the corresponding coordinates. Expressing the components of the vector $\boldsymbol{J} = (J_1, J_2, J_3)$ in terms of displacement, we have

$$J_1 = H_0\left(-\frac{\partial e}{\partial y} + \mu_0 \varepsilon_0 \ddot{v}\right),$$

$$J_2 = H_0\left(\frac{\partial e}{\partial x} - \mu_0\varepsilon_0\ddot{u}\right),$$

and $J_3 = 0$, by eliminating the quantities $\boldsymbol{h}$ and $\boldsymbol{E}$ from Eq. (1). Using the summation convection from Eqs. (7)–(10) we note that the third equation of motion in Eq. (12) is identically satisfied and first two equations become

$$\begin{aligned}
&\rho\left(\frac{\partial^2 u}{\partial t^2} - \Omega^2 u - 2\Omega\dot{v}\right)\\
&= A_{11}\frac{\partial^2 u}{\partial x^2} + B_2\frac{\partial^2 v}{\partial x\partial y} + B_1\frac{\partial^2 u}{\partial y^2} - \gamma\left(1+\nu_0\frac{\partial}{\partial t}\right)\frac{\partial T}{\partial x}\\
&\quad - \mu_0 H_0\frac{\partial h}{\partial x} - \varepsilon_0\mu_0^2 H_0^2\frac{\partial^2 u}{\partial t^2}, \qquad (14)\\
&\rho\left(\frac{\partial^2 v}{\partial t^2} - \Omega^2 v + 2\Omega\dot{u}\right)\\
&= A_{22}\frac{\partial^2 v}{\partial y^2} + B_2\frac{\partial^2 u}{\partial x\partial y} + B_1\frac{\partial^2 v}{\partial x^2}\\
&\quad - \gamma\left(1+\nu_0\frac{\partial}{\partial t}\right)\frac{\partial T}{\partial y}\mu_0 H_0\frac{\partial h}{\partial y} - \varepsilon_0\mu_0^2 H_0^2\frac{\partial^2 v}{\partial t^2}, \qquad (15)
\end{aligned}$$

where $B_1 = \mu_L$ and $B_2 = \alpha + \lambda + \mu_L$.

Equations (7)–(10) and (13)–(15) are the field equations of the generalized thermo-elasticity elastic solid. The theory of couple thermo-elasticity was extended by Lord and Shulman[33] and Green and Lindsay[34] through including the thermal relaxation time in constitutive relations. These theories eliminate the paradox of the infinite velocity of heat propagation and are termed generalized theories of thermoelasticity. The differences between the two theories are as follows.

(i) The Lord–Şulman (LS) theory involves one relaxation time of thermoelastic process (τ_0), while the Green and Lindsay (GL) theory involves two relaxation times (τ_0, ν_0).

(ii) The LS energy equation involves first and second time derivatives of strain, whereas the corresponding equation in the GL theory needs only the first time derivative of strain.

(iii) In the linearized case, according to the GL theory the heat cannot propagate at a finite speed unless the stresses depend on temperature velocity, whereas according to the LS theory the heat can propagate at a finite speed even though the stresses there are independent of temperature velocity.

(iv) The LS theory cannot be obtained from the GL theory.

Applied to the LS theory, the GL theory, as well as the classical coupled (CD) theory, is as follows:

i) The equations of the coupled thermo-elasticity CD theory, when

$$n_0 = 0, \quad n_1 = 1, \quad \text{and} \quad \tau_0 = \nu_0 = 0;$$

ii) Lord–Shulman (LS) theory, when

$$n_1 = n_0 = 1, \quad \nu_0 = 0, \quad \text{and} \quad \tau_0 > 0;$$

iii) Green–Lindsay (GL) theory, when

$$n_1 = 1, \quad n_0 = 0, \quad \text{and} \quad \nu_0 \geq \tau_0 > 0.$$

Particular cases:

iv) Neglecting angular velocity (i.e. $\Omega = 0$) in Eqs. (14) and(15), we obtain the transformed components of displacement, stress forces, and temperature distribution in a non-rotating generalized thermoelasticity medium.

v) Neglecting the effect of a magnetic field (i.e. $H_0 = 0$) in Eqs. (14) and (15), we obtain the transformed components of displacement, stress forces, and temperature distribution in a non-magnetic field generalized thermoelasticity medium.

For convenience, the following non-dimensional variables are used:

$$\begin{aligned}
&x' = c_1\eta x, \quad y' = c_1\eta y, \quad u' = c_1\eta u,\\
&v' = c_1\eta v, \quad t' = c_1^2\eta t, \quad \tau_0' = c_1^2\eta\tau_0,\\
&\theta = \gamma\frac{(T-T_0)}{\lambda+2\mu_T}, \quad \sigma_{ij}' = \frac{\sigma_{ij}}{\mu_T}, \quad \Omega' = \frac{\Omega}{c_1^2\eta},\\
&\tau'_0{=}c_1^2\eta\tau_0, \quad h' = \frac{h}{H_0}, \quad i,j = 1,2,
\end{aligned}$$

where

$$\eta = \frac{\rho C_E}{k} \quad \text{and} \quad c_1^2 = \frac{\lambda+2\mu_T}{\rho}. \qquad (16)$$

In terms of non-dimensional quantities defined in Eq. (16), the above governing equations reduce to (dropping the dashed for convenience)

$$\begin{aligned}
&\alpha_1\frac{\partial^2 u}{\partial t^2} - \Omega^2 u - 2\Omega\dot{v}\\
&= h_{11}\frac{\partial^2 u}{\partial x^2} + h_2\frac{\partial^2 v}{\partial x\partial y} + h_1\frac{\partial^2 u}{\partial y^2}\\
&\quad - \left(1+\nu_0\frac{\partial}{\partial t}\right)\frac{\partial\theta}{\partial x} - h_0\frac{\partial h}{\partial x}, \qquad (17)\\
&\alpha_1\frac{\partial^2 v}{\partial t^2} - \Omega^2 v + 2\Omega\dot{u}\\
&= h_{22}\frac{\partial^2 v}{\partial y^2} + h_2\frac{\partial^2 u}{\partial x\partial y} + h_1\frac{\partial^2 v}{\partial x^2}\\
&\quad - \left(1+\nu_0\frac{\partial}{\partial t}\right)\frac{\partial\theta}{\partial y} - h_0\frac{\partial h}{\partial y}, \qquad (18)
\end{aligned}$$

where

$$(h_{11}, h_{22}, h_1, h_2, h_0) = \frac{(A_{11}, A_{22}, B_1, B_2, \mu_0 H_0^2)}{(\lambda+2\mu_T)},$$

$$\alpha_1 = 1 + \frac{\varepsilon_0 \mu_0^2 H_0^2}{\rho},$$
$$(L_{11}, L_{22}, L_1, L_2) = (h_{11}, h_{22}, h_1, h_2) + h_0,$$
$$\varepsilon = \frac{\gamma^2 T_0}{\rho C_E (\lambda + 2\mu_T)}.$$

Using, $h = -H_0 e$ we obtain

$$\alpha_1 \frac{\partial^2 u}{\partial t^2} - \Omega^2 u - 2\Omega \dot{v} = L_{11} \frac{\partial^2 u}{\partial x^2} + L_2 \frac{\partial^2 v}{\partial x \partial y} + h_1 \frac{\partial^2 u}{\partial y^2} - \left(1 + \nu_0 \frac{\partial}{\partial t}\right) \frac{\partial \theta}{\partial x}, \quad (19)$$

$$\alpha_1 \frac{\partial^2 v}{\partial t^2} - \Omega^2 v - 2\Omega \dot{u} = L_{22} \frac{\partial^2 v}{\partial y^2} + L_2 \frac{\partial^2 u}{\partial x \partial y} + h_1 \frac{\partial^2 v}{\partial x^2} - \left(1 + \nu_0 \frac{\partial}{\partial t}\right) \frac{\partial \theta}{\partial y}, \quad (20)$$

$$\frac{\partial^2 \theta}{\partial x^2} + \frac{\partial^2 \theta}{\partial y^2} = \left(n_1 \frac{\partial}{\partial t} + \tau_0 \frac{\partial^2}{\partial t^2}\right) \theta + \varepsilon \left(n_1 \frac{\partial}{\partial t} + n_0 \tau_0 \frac{\partial^2}{\partial t^2}\right) \left(\frac{\partial u}{\partial x} + \frac{\partial v}{\partial y}\right), \quad (21)$$

$$\mu_T \sigma_{xx} = A_{11} u_{,x} + A_{12} v_{,y} - A_{22} \left(1 + \nu_0 \frac{\partial}{\partial t}\right) \theta, \quad (22)$$

$$\mu_T \sigma_{yy} = A_{22} v_{,y} + A_{12} u_{,x} - A_{22} \left(1 + \nu_0 \frac{\partial}{\partial t}\right) \theta, \quad (23)$$

$$\mu_T \sigma_{zz} = A_{12} u_{,x} + \lambda v_{,y} - A_{22} \left(1 + \nu_0 \frac{\partial}{\partial t}\right) \theta, \quad (24)$$

$$\mu_T \sigma_{xy} = \mu_L (u_{,y} + v_{,x}), \sigma_{zx} = \sigma_{zy} = 0. \quad (25)$$

3. Normal mode analysis

The normal mode analysis gives exact solutions without any assumed restrictions on temperature, displacement, and stress distributions. It is applied to a wide range of problems in different branches. The normal mode analysis is, in fact, to look for the solution in Fourier transformed domain. Assuming that all the field quantities are sufficiently smooth on the real line such that normal mode analysis of these functions exists.

The solution of the considered physical variable can be decomposed in terms of normal modes as the following form:

$$[u, v, \theta, \sigma_{ij}](x, y, t) = [u^*(x), v^*(x), \theta^*(x), \sigma_{ij}^*(x)] \exp(\omega t + \mathrm{i} a y), \quad (26)$$

where ω is the (complex) time constant, $\mathrm{i} = \sqrt{-1}$, a is the wave number in the y direction, and $u^*(x), v^*(x)$, $\theta^*(x)$, and $\sigma_{ij}^*(x)$ are the amplitude of the field quantities.

By using Eq. (26), then Eqs. (19)–(25) take the form

$$[L_{11} D^2 - A_1] u^* + [2\Omega\omega + \mathrm{i} a L_2 D] v^* = Q D \theta^*, \quad (27)$$

$$[h_1 D^2 - A_2] v^* + [-2\Omega\omega + \mathrm{i} a L_2 D] u^* = \mathrm{i} a Q \theta^*, \quad (28)$$

$$A_4 D u^* + \mathrm{i} a A_4 v^* = [D^2 - A_3] \theta^*, \quad (29)$$

$$\mu_T \sigma_{xx}^* = A_{11} D u^* + \mathrm{i} a A_{12} v^* - A_{22} Q \theta^*, \quad (30)$$

$$\mu_T \sigma_{yy}^* = A_{12} D u^* + \mathrm{i} a A_{22} v^* - A_{22} Q \theta^*, \quad (31)$$

$$\mu_T \sigma_{zz}^* = A_{12} D u^* + \mathrm{i} a \lambda v^* - A_{22} Q \theta^*, \quad (32)$$

$$\mu_T \sigma_{xy}^* = \mu_L (\mathrm{i} a u^* + D v^*), \sigma_{zx}^* = \sigma_{zy}^* = 0, \quad (33)$$

where

$$A_1 = \alpha_1 \omega^2 - \Omega^2 + h_1 a^2,$$
$$A_2 = \alpha_1 \omega^2 - \Omega^2 + L_{22} a^2, \quad Q = 1 + \omega \nu_0,$$
$$A_3 = a^2 + \omega(n_1 + \omega \tau_0),$$
$$A_4 = \omega \varepsilon (n_1 + n_0 \omega \tau_0), \quad D = \frac{\mathrm{d}}{\mathrm{d}x}.$$

Eliminating $\theta^*(x)$ and $v^*(x)$ in Eqs. (27)–(29), we obtain the partial differential equation satisfied by $u^*(x)$

$$[D^6 - A D^4 + B D^2 - C] u^*(x) = 0, \quad (34)$$

where

$$A = \frac{1}{h_1 h_{11}} \{L_{11} A_2 + h_1 A_1 + h_1 A_3 Q + h_1 L_{11} A_3 - L_2^2 a^2\}, \quad (35)$$

$$B = \frac{1}{h_1 h_{11}} \{A_1 A_2 + L_{11} A_2 A_3 + h_1 A_1 A_3 + Q(L_{11} a^2 A_4 + A_2 A_4 - 2 L_2 a^2 A_4) - L_2^2 a^2 A_3 + 4\Omega^2 \omega^2\}, \quad (36)$$

$$C = \frac{1}{h_1 L_{11}} \left\{A_1 A_2 A_3 + A_1 A_4 a^2 Q + 4\Omega^2 \omega^2 A_3\right\}. \quad (37)$$

In a similar manner, we can show that $v^*(x)$ and $\theta^*(x)$ satisfy the equation

$$[D^6 - A D^4 + B D^2 - C] \{v^*(x), \theta^*(x)\} = 0. \quad (38)$$

The above equation can be factorized as

$$\left(D^2 - k_1^2\right) \left(D^2 - k_2^2\right) \left(D^2 - k_3^2\right) u^*(x) = 0, \quad (39)$$

where k_n^2 $(n = 1, 2, 3)$ are the roots of the following characteristic equation:

$$K^6 - A K^4 + B K^2 - C = 0. \quad (40)$$

The solution of Eq. (33) which is bounded as $x \to \infty$, is given by

$$u^*(x) = \sum_{n=1}^{3} M_n(a, \omega) \exp(-k_n x). \quad (41)$$

Similarly

$$v^*(x) = \sum_{n=1}^{3} M'_n(a,\omega)\exp(-k_n x), \tag{42}$$

$$\theta^*(x) = \sum_{n=1}^{3} M''_n(a,\omega)\exp(-k_n x), \tag{43}$$

where $M_n(a,\omega)$, $M'_n(a,\omega)$, and $M''_n(a,\omega)$ are some parameters depending on a and ω.

Substituting Eqs. (42) and (43) into Eqs. (27)–(29), we have

$$M'_n(a,\omega) = H_{1n}M_n(a,\omega), \quad n=1,2,3, \tag{44}$$

$$M''_n(a,\omega) = H_{2n}M_n(a,\omega), \quad n=1,2,3. \tag{45}$$

Thus, we have

$$v^*(x) = \sum_{n=1}^{3} H_{1n}M_n(a,\omega)\exp(-k_n x), \tag{46}$$

$$\theta^*(x) = \sum_{n=1}^{3} H_{2n}M_n(a,\omega)\exp(-k_n x), \tag{47}$$

$$\sigma^*_{xx} = \sum_{n=1}^{3} H_{3n}M_n(a,\omega)\exp(-k_n x), \tag{48}$$

$$\sigma^*_{yy} = \sum_{n=1}^{3} H_{4n}M_n(a,\omega)\exp(-k_n x), \tag{49}$$

$$\sigma^*_{zz} = \sum_{n=1}^{3} H_{5n}M_n(a,\omega)\exp(-k_n x), \tag{50}$$

$$\sigma^*_{xy} = \sum_{n=1}^{3} H_{6n}M_n(a,\omega)\exp(-k_n x), \tag{51}$$

where

$$H_{1n} = \frac{\mathrm{i}aA_1 + \mathrm{i}aL_2k_n^2 - \mathrm{i}aL_{11}k_n^2}{L_2a^2k_n + h_1k_n^3 - A_2k_n}, \quad n=1,2,3, \tag{52}$$

$$H_{2n} = \frac{-L_{11}k_n^2 + A_1 + \mathrm{i}aL_2k_nH_{1n}}{k_n}, \quad n=1,2,3, \tag{53}$$

$$H_{3n} = \frac{-A_{11}k_n + \mathrm{i}aA_{12}H_{1n} - (\lambda+2\mu_T)H_{2n}}{\mu_T}, \quad n=1,2,3, \tag{54}$$

$$H_{4n} = \frac{-A_{12}k_n + \mathrm{i}aA_{22}H_{1n} - (\lambda+2\mu_T)H_{2n}}{\mu_T}, \quad n=1,2,3, \tag{55}$$

$$H_{5n} = \frac{-A_{12}k_n + \mathrm{i}a\lambda H_{1n} - (\lambda+2\mu_T)H_{2n}}{\mu_T}, \quad n=1,2,3, \tag{56}$$

$$H_{6n} = \frac{\mu_l(\mathrm{i}a - k_nH_{1n})}{\mu_T}, \quad n=1,2,3. \tag{57}$$

4. Application

In this section we need to consider the boundary conditions at $x=0$, in order to determine the parameters M_n $(n=1,2,3)$.

(I) Thermal boundary conditions that the surface of the half-space is subjected to thermal shock

$$\theta(0,y,t) = f(0.y,t) = f_0\exp(\omega t + \mathrm{i}ay). \tag{58}$$

(II) Mechanical boundary condition that surface of the half-space is traction-free

$$\sigma_{xx}(0,y,t) = \sigma_{xy}(0,y,t) = 0. \tag{59}$$

Substituting the expressions of the variables considered into the above boundary conditions, we can obtain the following equations satisfied by the parameters:

$$\sum_{n=1}^{3} H_{2n}M_n = f_0, \tag{60}$$

$$\sum_{n=1}^{3} H_{3n}M_n = 0, \tag{61}$$

$$\sum_{n=1}^{3} H_{6n}M_n = 0. \tag{62}$$

Solving Eqs. (59)–(61), we obtain the parameters M_n $(n=1,2,3)$ that are defined as follows:

$$M_1 = \frac{\Delta_1}{\Delta}, \quad M_2 = \frac{\Delta_2}{\Delta}, \quad M_3 = \frac{\Delta_3}{\Delta} \tag{63}$$

where

$$\begin{aligned}\Delta =\ & H_{21}(H_{32}H_{63} - H_{33}H_{62}) \\ & - H_{22}(H_{31}H_{63} - H_{61}H_{33}) \\ & + H_{23}(H_{31}H_{62} - H_{32}H_{61}),\end{aligned} \tag{64}$$

$$\Delta_1 = f_0(H_{32}H_{63} - H_{33}H_{62}), \tag{65}$$

$$\Delta_2 = -f_0(H_{31}H_{63} - H_{61}H_{33}), \tag{66}$$

$$\Delta_3 = f_0(H_{31}H_{62} - H_{32}H_{61}). \tag{67}$$

5. Numerical results

With a view to illustrating the analytical procedure presented earlier, we now consider a numerical example for which computational results are given. The results depict the variations of temperature, displacement, and stress fields in the context of three theories. To study the effects of rotation and reinforcement on wave propagation, we now present some numerical results for the physical constants.

$\lambda = 7.59\times10^9$ N/m^2, $\quad \mu_T = 1.89\times10^9$ N/m^2,
$\mu_L = 2.45\times10^9$ N/m^2, $\quad \alpha = -1.28\times10^9$ N/m^2,
$\beta = 0.32\times10^9$ N/m^2, $\quad \rho = 7800$ kg/m^2,

$\alpha_t = 1.78 \times 10^{-5}$ N/m^2, $k = 386$,
$C_E = 383.1$, $\tau_0 = 0.02$, $a = 1$,
$T_0 = 293$ K, $f^* = 1$, $\nu_0 = 0.03$,
$\omega = \omega_0 + \mathrm{i}\xi$, $\omega_0 = 2$, $\xi = 1$,
$C_E = 383.1$ J/(kg $\cdot$ K), and
$\mu = 3.86 \times 10^{10}$ kg/ms^2.

The computations are carried out for a value of time $t = 0.1$. The numerical technique, outlined above, is used for the distribution of the real part of the thermal temperature θ, the displacements u and v, the stress σ_{xx}, σ_{yy}, and σ_{xy} distributions for the problem. The field quantities, temperature, displacement components u, v, and stress components σ_{xx}, σ_{yy}, and σ_{xy} depend not only on space x and time t but also on the thermal relaxation time τ_0 and ν_0. Here all the variables are taken in nondimensional forms. When there exist two thermal relaxation times for two different values of magnetic field and rotation (i.e. in the absence and the presence of magnetic field and rotation) the results are shown in Figs. 1–18. These figures each show the three curves predicted by different theories of thermoelasticity. In these figures, the solid lines represent the solutions in the coupled theory, the dotted lines denote the solutions in the generalized LS theory and dashed lines refer to the solutions derived using the GL theory. We notice that the results for the temperature, the displacement, and stresses distribution when the relaxation time is included in the heat equation are distinctly different from those when the relaxation time is not considered in the heat equation, because the thermal waves in the Fourier's theory of heat equation travel at an infinite speed of propagation as opposed to finite speed in the non-Fourier case. This demonstrates clearly the difference between the coupled theory and the generalized theory of thermoelasticity. For the value of y, $y = 1$ is used in performing the computation. Figures 1–6 show the comparisons between the temperature θ, the displacement components u, v, the force stresses components σ_{xx}, σ_{yy}, and σ_{xz}, the case of different two values of rotation and a magnetic field under three theories. It should be noted in Fig. 1 that under the influence of a magnetic field and rotation θ values first decrease to their minimal values at the beginning, then smoothly increase to their maximal values and increase with tacking the wave behaviours. The values of temperature quantity converge to zero with distance x increasing. The effects of rotation and the magnetic field on temperature increase the amplitudes of θ's, which displays the nature of the medium with rotation under the influence of magnetic field. But in the case of no magnetic field and rotation the temperatures increase in the beginning to their maximal amplitudes then smoothly decrease, and also moves in the wave propagation. The values of temperature quantity converges to zero with distance x increasing.

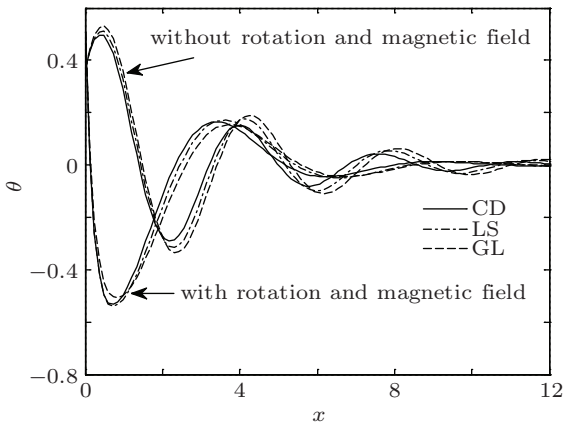


Fig. 1. Temperature (θ) distributions at different values of magnetic field and rotation.

Figure 2 shows that in the presence of the magnetic field and rotation, horizontal displacements u's begin from the negative values and then to their maximal amplitudes and also move in the wave propagation. In the absence of the magnetic field and rotation displacement curves always start from the negative values and terminate at the zero value, i.e., they first smoothly increases to their maxima, then they fall again to try to retain zero at infinity. The effects of the magnetic field and rotation as illustrated in the figure make the values of u's for the case with magnetic field and rotation smaller than those for the case without them. Behaviours of displacement u's in CD, LS, and GL theories for two different values of magnetic field and rotation are similar in two cases. Figure 3 shows the vertical displacement v's. We can see that displacement component v's always start from positive values and terminate at the zero value without and with a magnetic field and rotation: they sharply increase in the beginning to their maximal amplitudes and smoothly decrease in the two cases. When the magnetic field and rotation are present, the v's start from the positive values and terminate at the zero value but v's always start from the positive values and smoothly decrease in the beginning to the minimum amplitudes then smoothly increase. Also v's

in this case reach their minimal values, finally reaching zero at infinity (state of particles equilibrium). The displacements u and v show different behaviours, because of the elasticity of the solid tends to resist vertical displacementin the problem under investigation. The stress components σ_{xx}'s reach zero value (Fig. 4) and satisfy the boundary condition at $x = 0$, start sharply increase and reach the maximal values in the two cases and then smoothly decrease and converge to zero with distance x increasing, the behaviours of three theories are similar (i.e. different values of relaxation time). In the case, when the magnetic field and rotation are absent, the stress components increase at the start then decrease to the zero value with the increase of distance in the context of the three theories. These trends obey the elastic and thermoelastic properties of the solid under investigation. Figure 5 shows that the stress components σ_{yy}'s have the same behaviours in the absence and the presence of magnetic field and rotation. When magnetic field and rotation are absent the stress components first increase to their maximal values then decrease to their minimal values, and reach zero at infinity in the context of the three theories, but when the magnetic field and rotation are present, the stress components first increase then decrease and reach the zero value in the context of the three theories. These trends obey the elastic and thermoelastic properties of the solid under investigation. Figure 6 shows that the stress components σ_{xy}'s satisfy the boundary condition, and when the magnetic field and rotation are present, they sharply decrease to their minimal values, then increase to their maximal values but when the magnetic field and rotation are absent the stress components exhibit almost the same behaviours as when the magnetic field and rotation are present. The lines without the magnetic field and rotation have lower gradient than with the magnetic field and rotation. These trends obey the elastic and thermoelastic properties of the solid.

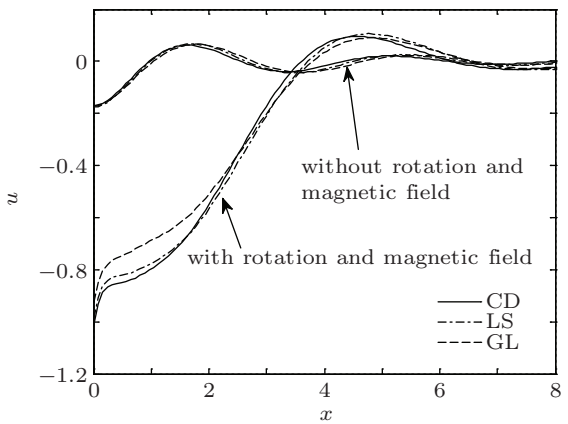


Fig. 2. Horizontal displacement (u) distributions at different values of magnetic field and rotation.

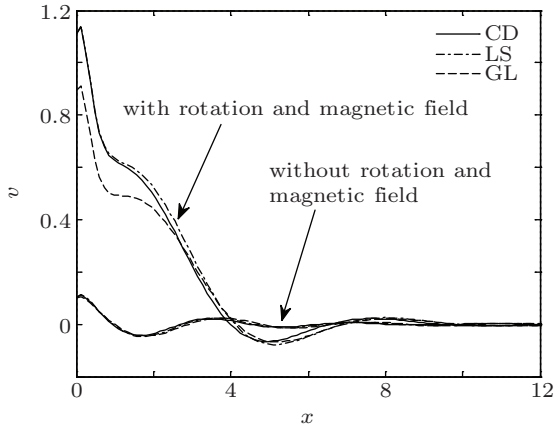


Fig. 3. Vertical displacement (v) distributions at different values of magnetic field and rotation.

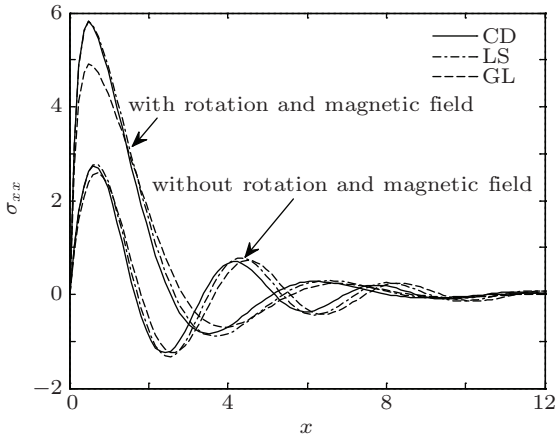


Fig. 4. Distributions of stress components σ_{xx}'s at different values of magnetic field and rotation.

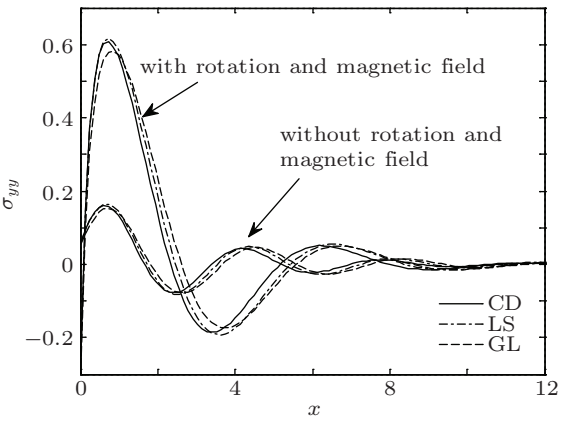


Fig. 5. Distributions of stress components σ_{yy}'s at different values of magnetic field and rotation.

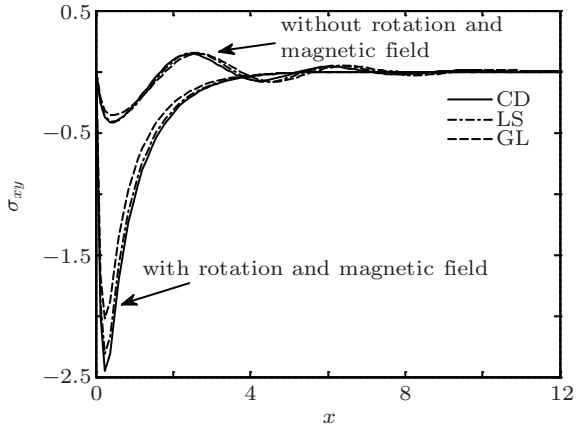


Fig. 6. Distributions of stress components σ_{xy}'s at different values of magnetic field and rotation.

Figures 7–12 show the comparisons between temperature θ's, displacement components u's, v's, the force stress components σ_{xx}'s, σ_{yy}'s, and σ_{xy}'s, in the cases of two different values of rotation and magnetic field under three theories. It should be noted in Fig. 7 that in this problem θ's first decrease to their minimum value then smoothly increase (with maximal positive gradients). Graph lines for both values of rotation show different slopes. In other words, the temperature lines for $\Omega = 0.0$ have higher gradients than those for $\Omega = 0.2$ in the range $1.1 \leq x \leq 4$ but smaller in the ranges $0 \leq x \leq 1.1$ and $4 \leq x \leq 7$. In addition, all lines begin to coincide when the horizontal distance x increases to the reference temperature of the solid. These results obey physical reality for the behaviour of fiber as a polycrystalline solid. Figure 8 shows the horizontal displacements u's, despite the peaks (for different values of rotation) occurring at equal values of magnetic field, the magnitude of the maxiaml displacement peak strongly depends on the rotation. It is also clear that the rates of change of u's increase with rotation increasing. On the other hand, Fig. 9 shows that the vertical displacements v's, first increase near the beginning, then decrease to minimal values and reach zero value at the infinity (state of particles equilibrium). Figure 10 shows the horizontal stress components σ_{xx}'s. The curves for both values of rotation and magnetic field show different slopes. In other words, the σ_{xx} component curves for $\Omega = 0.0$ have higher gradients than those for $\Omega = 0.2$ in the range $1.1 \leq x \leq 4$ but lower in all other ranges. In addition, all curves begin to coincide when the horizontal distance x increases to zero after their relaxations at infinity. Variation of Ω has a serious effect on both magnitudes of mechanical stresses. These trends obey the elastic and thermoelastic properties of the solid under investigation. Figure 11 shows the stress components σ_{yy}'s, which take the same behaviours as those in Fig. 10. Figure 12 shows that the stress components σ_{xy}'s satisfy the boundary condition, they first sharply decrease and then increase to their maximal values in the context of the $\Omega = 0.2$ and in the case of $\Omega = 0.0$ they take the same

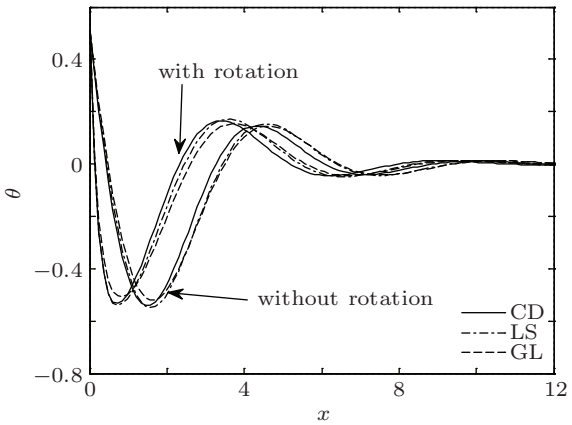


Fig. 7. Temperature (θ) distributions at different values of rotation.

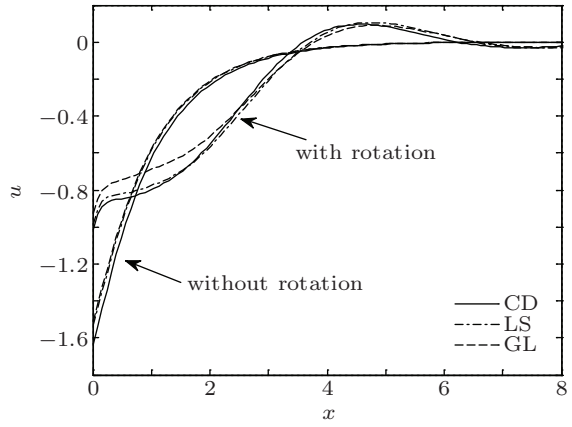


Fig. 8. Horizontal displacement (u) distributions at different values of rotation.

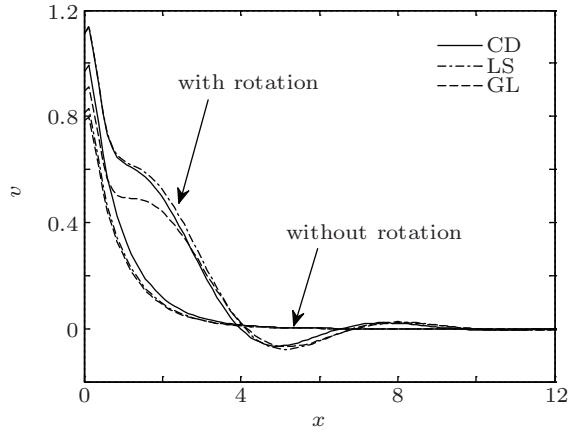


Fig. 9. Vertical displacement (v) distributions at different values of rotation.

behaviors as in the case of $\Omega = 0.2$. The curves for $\Omega = 0.0$ have higher gradients than those for $\Omega = 0.2$ and take the exponential behaviours but when the rotation is present they present the wave propagation. These trends obey the elastic and thermoelastic properties of the solid.

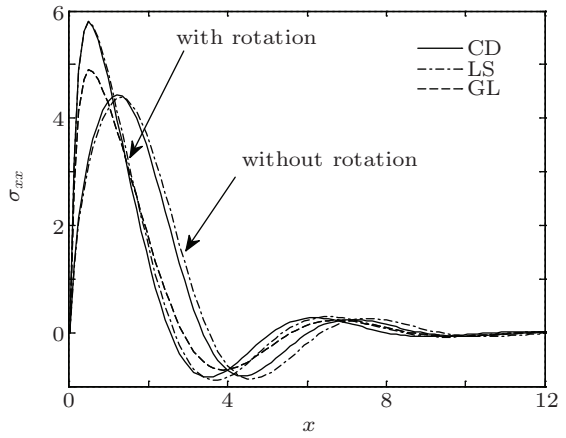


Fig. 10. Distributions of stress components σ_{xx}'s at different values of rotation.

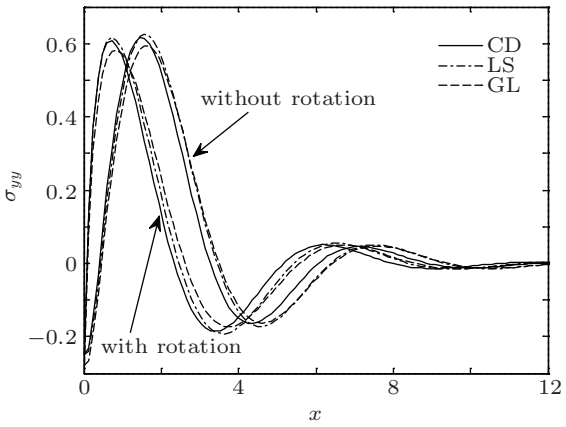


Fig. 11. Distributions of stress components σ_{yy}'s at different values of rotation.

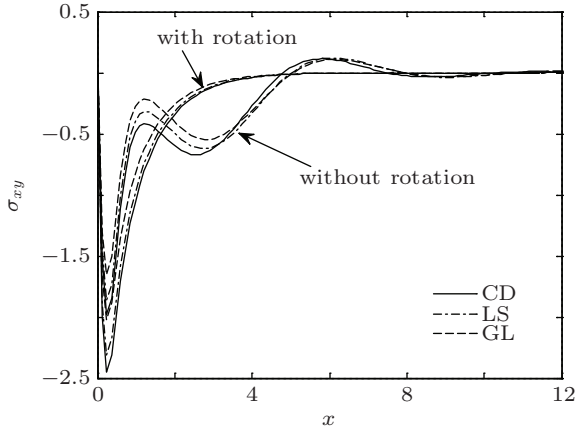


Fig. 12. Distributions of stress components σ_{xy}'s at different values of rotation.

Figures 13–18 show the comparisons between temperature θ's, displacement component u's, v's, the force stress components σ_{xx}'s, σ_{yy}'s, and σ_{xy}'s, for the cases of two different values of magnetic field and rotation ($\Omega = 0.2$) under three theories.

It should be noted in Fig. 13 that in the presence of magnetic field θ's first decrease to their maximal values then increase with tacking the wave behaviours. However, in the absence of a magnetic field the temperature take the same behaviours as in the presence of a magnetic field and also present wave propagation. The values of temperature converge to zero with the increase of distance x. The effect of the magnetic field on temperature reduces the value of amplitude of θ, which is the nature for the medium with a magnetic field. Figure 14 exhibits that in the presence of a magnetic field the horizontal displacements u's, beginning from their negative values then increasing to their maximal amplitudes, also present wave propagation. However in the absence of a magnetic field the horizontal displacements start from their negative values and terminate at the zero value: they first smoothly decrease to their minima, then increase to their maxima, afterwards u's fall again to try to retain zero at infinity but the effects in the presence of magnetic field illustrated in the figure show that the values of u's in the presence of a magnetic field are smaller than those in the absence of magnetic field in some ranges. The behaviours of displacements, u's in CD, LS, and GL theories for two different values of magnetic field are nearly similar in two cases. Figure 15 shows that the vertical displacements v's, always start from positive values and terminate at a zero value but in the absence of a magnetic field v's always start from positive values then sharply increase from the beginning to their maximal amplitudes then smoothly decrease. However, in the presence of a magnetic field, v's start from their positive values and terminate at the zero value but v's always start from their positive values and sharply increase in the beginning to their maximal amplitudes then smoothly decrease. Also v's in this case reach minimal values, then reach zero value at the infinity (state of particles equilibrium). The displacements u's and v's show different behaviours, because the elasticity of the solid tends to resist vertical displacements in the problem under investigation. Figure 16 explains that the stress components σ_{xx}'s reach coincidence with zero value and satisfy the boundary condition at $x = 0$, start to sharply increase and reach their maximal values in two cases

and converge to zero with the increase of distance x, behaviours of three theories are similar. In the case of no magnetic field, σ_{xx}'s increase in the start then decrease and reach the zero value with the increase of distance in the context of the three theories. These trends obey the elastic and thermoelastic properties of the solid under investigation. The magnetic field causes the relaxation of the wave propagation and increase their amplitudes of the stress value. Figure 17 shows that the stress components σ_{yy}'s have the same behaviours in the presence and the absence of a magnetic field. In the absence of a magnetic field, they first increase in the start then decrease to their minima and propagate until reaching the zero value at infinity in the context of the three theories. These trends obey the elastic and thermoelastic properties of the solid under investigation. Figure 18 shows that the stress components σ_{xy}'s satisfy the boundary condition, in the presence of magnetic field they sharply decrease in the start then increase but in the absence of magnetic field σ_{xy}'s have nearly the same behaviours as those in the presence of magnetic field. The curves in the absence of magnetic field have higher gradients than those in the presence of magnetic field. These trends obey the elastic and thermoelastic properties of the solid.

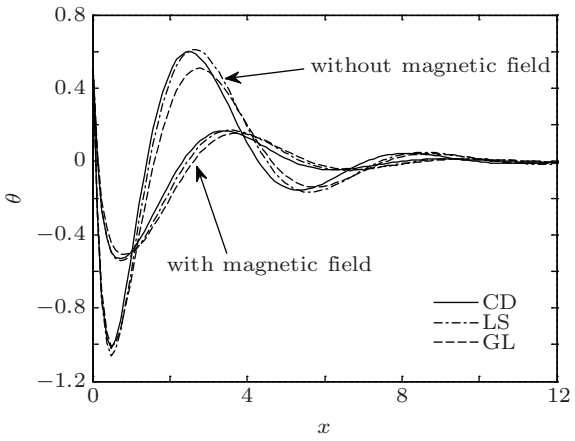


Fig. 13. Temperature (θ) distributions at different values of magnetic field.

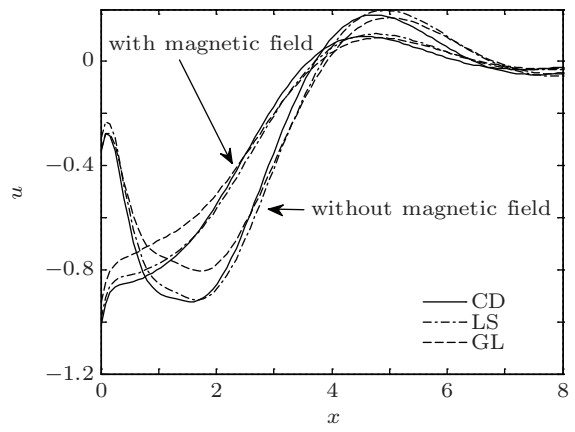


Fig. 14. Horizontal displacement (u) distributions at different values of magnetic field.

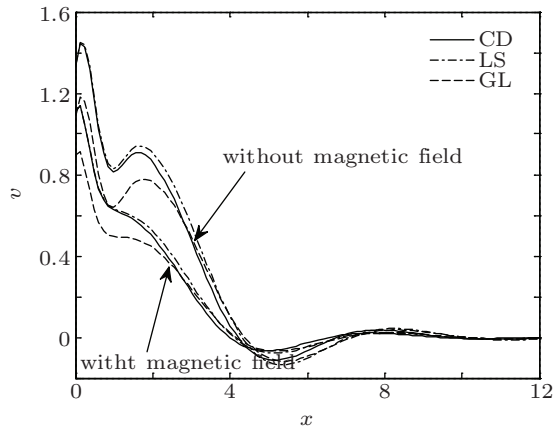


Fig. 15. Vertical displacement (v) distributions at different values of magnetic field.

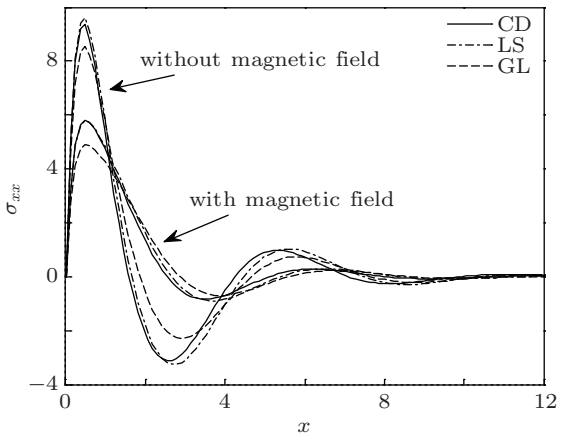


Fig. 16. Distribution of stress components σ_{xx}'s at different values of magnetic field.

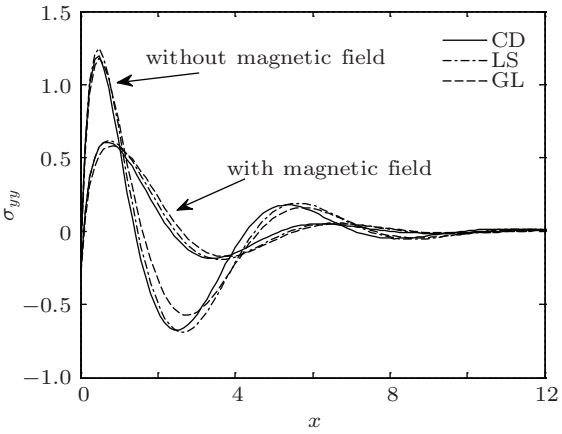


Fig. 17. Distributions of stress components σ_{yy}'s at different values of magnetic field.

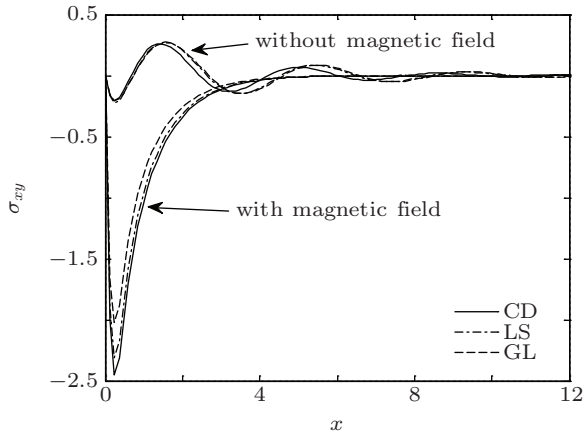


Fig. 18. Distributions of stress components σ_{xy}'s at different values of magnetic field.

6. Conclusion

I) The curves of the physical quantities under the CD theory in most figures are lower than those under the LS theory and the GL theory, owing to the relaxation times.

II) Analytical solutions based on normal mode analysis of the themoelastic problem in solids are developed and utilized.

III) A change of volume is accompanied by a change of the temperature while the effect of the deformation on the temperature distribution is the subject of the theory of thermoelasticity.

IV) The values of all the physical quantities converge to zero with the increase of distance x and all functions are continuous.

V) The fibre reinforcement has an important influence on the distribution of the field quantities.

VI) The method that is used in the present article is applicable to a wide range of problems in thermodynamics and thermoelasticity.

VII) The presence of a magnetic field plays a significant role in all the physical quantities. The amplitudes of all the physical quantities decrease while the rotation and gravity increase. Therefore, the presence of rotation and influence of gravity in the current model are of significance.

VIII) The deformation of a body depends on the nature of applied force as well as the type of boundary conditions.

VX) The presence of rotation has a significant influence on all the physical quantities. The amplitudes of all the physical quantities decrease while the rotation increases. Therefore, the presence of rotation in the current model is of significance.

References

[1] Othman M I A 2008 *Multi. Modeling in Materials and Structures* **1** 231

[2] Othman M I A and Song Y 2008 *Appl. Math. Modelling* **32** 811

[3] Paria G 1967 *Adv. Appl. Mech.* **10** 73

[4] Belfield A J, Rogers T G and Spencer A J M 1983 *J. Mech. Phys. Solids* **31** 25

[5] Verma P D S and Rana O H 1983 *Mech. Materials* **2** 353

[6] Singh S J 2002 *Sãdhanã* **27** 1

[7] Sengupta P R and Nath S 2001 *Sãdhanã* **26** 363

[8] Hashin Z and Rosen W B 1964 *J. Appl. Mech.* **31** 223

[9] Singh B and Singh S J 2004 *Sãdhanã* **29** 249

[10] Chattopadhyay A and Choudhury S 1990 *Int. J. Eng. Sci.* **28** 485

[11] Chaudhary S, Kaushik V P and Tomar S K 2004 *Acta Geoph. Polonica* **52** 219

[12] Chattopadhyay A and Choudhury S 1995 *Int. J. Num. Anal. Meth. Geomech.* **19** 289

[13] Pradhan A S, Samal K and Mahanti N C 2003 *Tamkang J. Sci. Eng.* **6:3** 173

[14] Chattopadhyay A, Venkateswarlu R L K and Saha S 2002 *Sãdhanã* **27** 613

[15] Othman M I A and Song Y 2007 *Int. J. Sol. & Struc.* **44** 5651

[16] Verma P D S, Rana O H and Verma M 1988 *Indian J. Pure Appl. Math.* **19** 713

[17] Singh B 2006 *Arch. Appl. Mech.* **75** 513

[18] Verma P D S 1986 *Int. J. Eng. Sci.* **24** 1067

[19] Ezzat M and Othman M I A 2002 *J. Thermal Stresses* **25** 409

[20] Sherief H H and Helmy K A 2002 *Int. J. Eng. Sci.* **40** 587

[21] Roy Choudhuri S K and Mukhopadhyay S 2000 *Int. J. Math. Sci.* **23** 479

[22] Othman M I A, Lotfy K H and Farouk R M 2009 *Acta Phys. Polonica* A **116** 186

[23] Ezzat M and Othman M I A 2000 *Int. J. Engng. Sci.* **38** 107

[24] Othman M I A 2010 *Mechanics and Mechanical Engineering* **14** 31

[25] Othman M I A 2004 *Acta Mechanica* **169** 37

[26] Roy Choudhuri S K 1990 *Comput. Math. Appl.* **19** 85

[27] Lotfy K H 2012 *Chin. Phys.* B **21** 014209

[28] Roy Choudhuri S K and Debnath L 1985 *J. Elasticity* **15** 59

[29] Othman M I A and Lotfy K H 2009 *MMMS* **5** 235

[30] Lotfy K H 2011 *Chin. Phys.* B **20** 074601

[31] Othman M I A and Lotfy K H 2010 *Int. Commun. Heat Mass Transfer* **37** 192

[32] Othman M I A and Lotfy K H 2009 *Int. J. Ind. Math.* **2** 87

[33] Lord H W and Şhulman Y A 1967 *J. Mech. Phys. Solid* **15** 299

[34] Green A E and Lindsay K A 1972 *J. Elasticity* **2** 1